Development of Dispersed Phase Size and Its Dependence on Processing Parameters

Xi Chen, Jun Xu, Bao-Hua Guo

Institute of Polymer Science and Engineering, Department of Chemical Engineering, Tsinghua University, Beijing 100084, People's Republic of China

Received 31 July 2005; accepted 9 January 2006
DOI 10.1002/app.24551
Published online in Wiley InterScience (www.interscience.wiley.com).

ABSTRACT: Through measurement of phase dimension via laser scattering, phase morphology development in immiscible blends of polyamide 12/poly(ethylene glycol) (PEG) with an extremely high viscosity ratio was investigated. The blends were prepared by melt blending in a batch mixer. The objective was to examine the influence of mixing time, rotor speed, as well as blending temperature on the size distribution of the minor phase. It is of interest that the breakup process of the dispersed PA 12 phase was observed for the blend systems even for extremely high viscosity ratios of $\leq 10^2$–10^3. Mixing time had a significant effect on the development of dispersed phase size distribution. It was found that the bulk of particle size reduction took place very early in the mixing process, and very small droplets with a diameter of 0.1–10 μm were produced. The number of small particles then decreased, resulting in a larger average particle size. With further prolonged mixing, the particle size levels off. The particle size and its distribution were also found to be sensitive to the rotor speed. The average particle size decreased with increased rotor speed. The effect of blending temperature on size and size distribution, which has seldom been studied, was also examined in this work. When the blending temperature altered from 190°C to 220°C, the size and its distribution of the dispersed phase varied considerably, and the change of viscosity ratio was found to be the key factor affecting the dispersed phase size. © 2006 Wiley Periodicals, Inc. J Appl Polym Sci 102: 3201–3211, 2006

Key words: polymer blends; particle size; viscosity

INTRODUCTION

Blending of two or more polymers has proved a useful and important alternative method of developing new materials with improved properties. Optimization of properties that is hard to obtain in a single homopolymer or copolymer can be achieved in polymer blends. When two polymers are mixed together, the minor phase tends to form spherical drops dispersed in the major matrix phase. It is commonly established that the final property of an immiscible polymer with spherical morphology is controlled by the size and size distribution of the dispersed phase.[1,2] Therefore, it is very important to study the relationship between the processing conditions and the multiphase morphology. The morphology development of the blend phase has been studied in many articles. The steady-state morphology is generally considered as the result of dynamic equilibrium between the breakup of droplets and their coalescence.[3,4] Further understanding of the process of drop breakup and coalescence is also necessary for better design and control of morphology of immiscible polymer blends.

Correspondence to: B.-H. Guo (bhguo@mail.tsinghua.edu.cn).

Journal of Applied Polymer Science, Vol. 102, 3201–3211 (2006)

During the processing of polymer blends, several factors are critical in determining the final size and size distribution of minor phase: composition, interfacial tension, viscosity ratio, elasticity ratio, and processing conditions, including time of mixing, speed of rotor or screw, and type of mixer. Many investigations[5–15] have been undertaken to understand the dependence of the phase size of polymer blends on the processing conditions. Several models were also proposed to simulate the dispersion process and predict the size of the dispersed phase.

Taylor[16,17] conducted an in-depth investigation of the breakup and disintegration of a Newton fluid. According to his theory, a relationship was put forward to predict the maximum drop size that could be stable in Newtonian blends system under simple shear flow. The equilibrium drop size will be reached when the shear forces deforming the drops are equal to the interfacial forces stabilizing the drops:

$$D_{\text{Taylor}} = \frac{\sigma}{\eta_m \dot{\gamma}} \frac{16\eta_r + 16}{19\eta_r + 16} \tag{1}$$

where D_{Taylor} is the predicted diameter of dispersed phase according to Taylor's theory, σ is the interfacial tension, $\dot{\gamma}$ is the shear rate, η_m is the viscosity of matrix phase, and η_r is the viscosity ratio.

However, the extension of Taylor's theory to a viscoelastic system such as polymer blends under an extension flow is difficult. This is because the elasticity of components will also have considerable influence on the dispersion process, and an elongational flow field has proved more effective than a shear flow field.[18] After studying eight blends of nylon or PET/Ethylene-propylene rubber, Wu[11] came to the conclusion that the closer the viscosities of the components, the smaller the particles that would be generated. In addition, a master curve between the Webber number and the viscosity ratio was fitted; hence, the influence of viscosity ratio and interfacial tension on the dispersed phase size was obtained in the following empirical equation:

$$D_{\mathrm{Wu}} = 4\eta_r^{\pm 0.84}\frac{\sigma}{\eta_m\dot{\gamma}} \tag{2}$$

where D_{Wu} is the predicted diameter of dispersed phase according to Wu's theory. When η_r is > 1, the exponent is positive, and it is negative if η_r is < 1. The Wu equation takes into account the coalescence process, but not the composition effect, although it was developed for blends with a fixed composition at 15 wt % of the disperse phase.[11,16,17] In fact, a dispersed phase content of 0.5–1 wt % was found to be adequate to induce coalescence.[3,4] Nevertheless, both equations indicated that the diameter of dispersed particles was inversely proportional to the shear rate as long as the variation of viscosity ratio with shear rate could be neglected.

Fortelny et al.[12] took into account both the influence of coalescence and blend composition and modified the precedents' work. By taking the final size of the minor phase as the results of the equilibrium built between the process of breakup and coalescence, Fortelny's group established a new relationship to predict the steady-state drop diameter:

$$D_{\mathrm{Fortelny}} = \frac{2\sigma(Ca)_{\mathrm{crit}}}{\eta_m\dot{\gamma}} + \frac{8\sigma P_{\mathrm{coal}}}{\pi\eta_m f_1}\phi_d \tag{3}$$

where D_{Fortelny} is the predicted diameter of dispersed phase according to Fortelny's theory. The first term on the right represents the critical droplet diameter calculated from critical capillary number. P_{coal} is the probability that droplets will coalesce after their collision, f_1 is the slope of the function describing the frequency of breakups of droplets at the critical value of Weber number for the droplet breakup, and ϕ_d is the volume fraction of the dispersed phase. It is difficult to quantify some of the parameters for the polymer blends contained in this equation, so its application is somewhat limited.

Many investigations on the morphology development have been carried out,[19–28] but these works have focused primarily on binary blends with a viscosity ratio of $0.01 \sim 20$, and have only put forward limited quantitative analysis of the relationship between morphology development and processing conditions. For the case of an extreme viscosity ratio, few discussions have been reported.

In our study, a blend with an extremely high viscosity ratio, Nylon 12/PEG is investigated as a model system. The objective is to present a quantitative analysis of the phase morphology development in Nylon 12/PEG blends as a function of the mixing time, rotor speed, and blending temperature. The good water dissolvability of PEG enables us to separate nylon from the blends conveniently, and a new method is used to perform measurement of phase dimension. This blend system with extremely high viscosity ratio is found to behave differently from that reported in previous literature during morphology development. The obtained results are compared with the existing models, and some modification is made.

EXPERMENTAL

Materials

Commercial-grade Nylon 12 was purchased from UBE Industries (Yamaguchi, Japan), and used as received. Poly(ethylene glycol) (PEG) with a molecular weight Mw of 20,000 was provided by Beijing Huiyou Chemical Corporation (Beijing, People's Republic of China).

Preparation of blends

Before a typical mixing experiment Nylon 12 was dried at 80°C for 12 h and PEG was dried under vacuum at 40°C for 8 h to minimize hydrolytic degradation of the polyamide during processing. The Nylon 12 pellets and PEG powder were then pre-mixed and melt-blended in a ThermoHaake Rheomix 600p. The total weight of the materials in the chamber was kept constant at 56 g.

When the specified mixing process was finished, the melt was rapidly poured into cold water to quench it and eliminate any further morphology change of nylon droplets. After the PEG was dissolved in the water, Nylon 12 particles were separated and ready for analysis.

Morphological analysis

Optical microscopy

The sample was quenched by cool water, and the PEG was then dissolved. The particles of Nylon 12 was suspended in the PEG solution and observed under brightfield conditions. The microscope used was Olympus BH-2. Images was photographed and recorded by the B/W CCD camera (Sanyo, Osaka, Japan) connected to the computer.

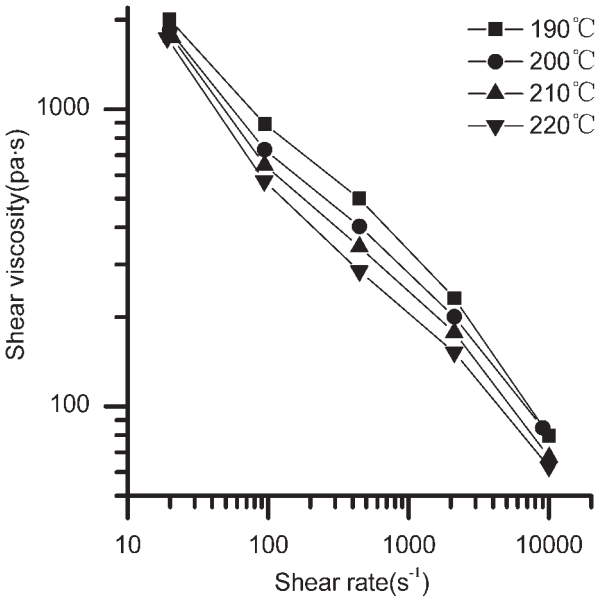

Figure 1 Shear viscosity of Nylon 12 at different temperature.

Size and size distribution analysis

Primarily scanning electron micrographs (SEMs) and Image Analysis Software were used in the morphological analysis. Since SEMs only provide information on limited numbers of particle morphology perpendicular to the microtoming direction, this method is not precise enough to wholly reflect the size and size distribution of the minor phase. Although various solutions to the problems of the determination of the size and size distribution of spherical particles from measurements made on random plane sections have appeared in the literature, in many cases the solutions have an unrealistic particle model or a mathematically complex one. Different from the previous methods for the size measurements, a Particle Characterization System, Malvern Mastersizer (produced by Malvern Co. British, Worcestershire, United Kingdom) was used in our study to measure the size and size distribution of Nylon 12 particles. Samples were put into water, and the PEG phase was selectively dissolved, leaving the Nylon 12 particles suspended in the water. The suspension was analyzed directly by the Malvern Mastersizer. Using the laser-scattering principles and refractive index difference between the various substances, this instrument can produce a quick and precise measurement of the size and size distribution of particles suspended in water or other solvents. The volume average particle diameter and uniformity can be conveniently obtained, and the results exhibit good reproducibility.

Volume average diameter is described as follows:

$$D_v = \left[\frac{\sum V_i d_i}{\sum Vi}\right] \tag{4}$$

where V_i is the relative volume in class i with a mean diameter of d_i.

Uniformity is used to characterize the broadness of the size distribution, calculated by using the following equation:

$$\text{Uniformity} = \frac{\sum V_i |d(x, 0.5) - d_i|}{d(x, 0.5) \sum V_i} \tag{5}$$

where $d(x, 0.5)$ is the median size of the distribution, and d_i and V_i are, respectively, the mean diameter of, and relative volume of class i. This coefficient can characterize breadth of size distribution and degree of particle uniformity.

Rheological measurements

Rheological measurement of Nylon 12 was carried out in an Rh-2000 Rheometer with an L/D ratio of 16 and an entry angle of 90°. The Bagley correction was made. Viscosity measurement of PEG was performed in a coaxial cylinder rheometer MCR 300 with a temperature of 80–100°C. The internal rotor radius was 13.33 mm, and the stationary cylinder radius was 14.46 mm. The shear rates were set within the range of 0.1–100 S^{-1}. As it is difficult to heat the sample to a temperature of > 100°C in the MCR 300 rheometer used, the viscosity of PEG at a higher temperature was obtained by calculation with the Arrhenius equation: $\eta = Ae^{\Delta E_\eta / RT}$.

RESULTS AND DISCUSSION

Rheological properties

The melt viscosities of the Nylon 12 are plotted as a function of shear rate at 190°, 200°, 210°, and 220°C in Figure 1. In the double logarithmic plot, Nylon 12 gives approximately straight lines between the entire shear rates from 20 s^{-1} to 10,000 s^{-1}. The curves for Nylon 12 may be roughly expressed by the power law

$$\eta = \eta_0 \dot{\gamma}^{\alpha} \tag{6}$$

where η is the melt viscosity, $\dot{\gamma}$ is the shear rate, and η_0 and α are constants. The fitting results of the data from the capillary rheometer were used to estimate the shear

TABLE I
Nylon 12 Viscosity at 190–220°C and Different Shear Rate Calculated

Rotor speed (rpm)	γ (s^{-1})	η_a (Pa s)			
		190°C	200°C	210°C	220°C
50	37.4	1528	1292	1199	1081
75	56.0	1247	1062	977	879
100	74.7	1079	923	845	759
125	93.4	965	8289	755	677
150	112	880	7589	689	617
175	131	815	704	637	571
200	149	762	660	596	533

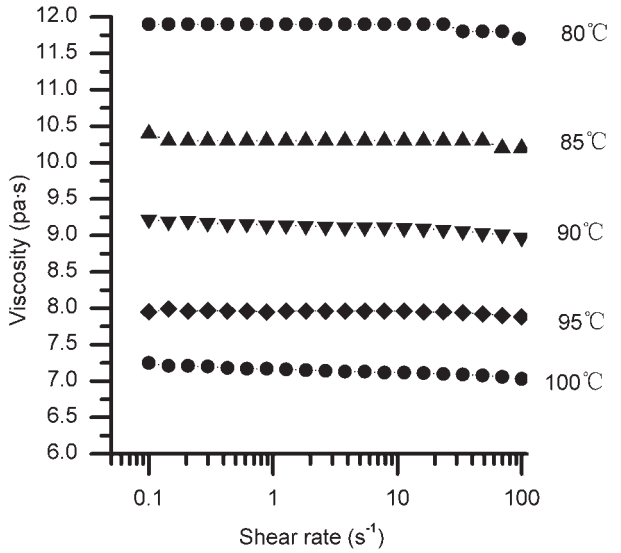

Figure 2 Viscosity of PEG at different temperatures.

viscosities of Nylon 12 at specific shear rates in the ThermoHaake Rheomix, which are listed in Table I. The expression used to estimate shear rate from the rotor speed is illustrated in the Appendix.

The shear viscosity of PEG at five temperatures (80°, 85°, 90°, 95°, and 100°C) is shown in Figure 2. The viscosity remained at almost the same value when the shear rate increased from 0.1 s^{-1} to 100 s^{-1} at a fixed temperature, so we can rationally presume that PEG performed as a Newtonian liquid in our experiment. The plotted results of viscosity at a shear rate of 0.1 s^{-1} versus temperature in Figure 3 show that they were in a strict agreement to the Arrhenius equation:

$$\eta = Ae^{\Delta E_\eta / RT} \tag{7}$$

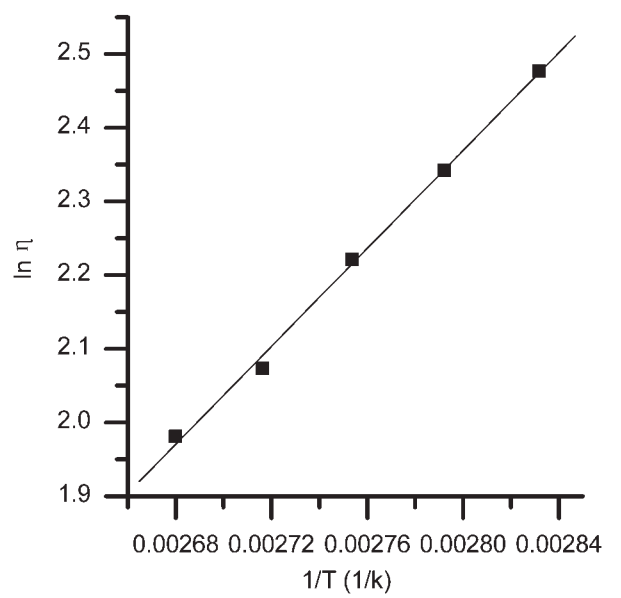

Figure 3 Fitting of the PEG viscosity vs. temperature.

TABLE II
Calculated PEG Viscosity at Higher Temperature

T (°C)	Viscosity (Pa s)
190	1.275
200	1.093
210	0.947
220	0.824

where η is the melt viscosity, T is the temperature, ΔE_η is the flow activation energy reflecting the flowing ability of polymers, and A is a constant. Therefore, the viscosity of PEG at a higher temperature can be predicted by using the equation obtained from the linear fitting result. Its viscosity at a higher temperature is listed in Table II.

With the viscosity of Nylon 12 and PEG obtained, we acquired the viscosity ratio of the system at a different temperature and shear rate, as shown in Figure 4. The viscosity ratio of our system was in the magnitude of $10^2 \sim 10^3$, and it was lower at 190°C than at 200 ~ 220°C.

Effect of mixing time on minor phase size and distribution

The morphology development of a binary immiscible polymer blends has been studied and is crudely described in Figure 5 as discussed in some investigations.[4,5,13] Under shearing or extensional flow, the initial molten pellets undergo transient affine deformation to form sheets or threads. The latter will break up into small particles due to the interfacial instability. These particles may coalesce with each other because of the interfacial tension and grow into larger particles.

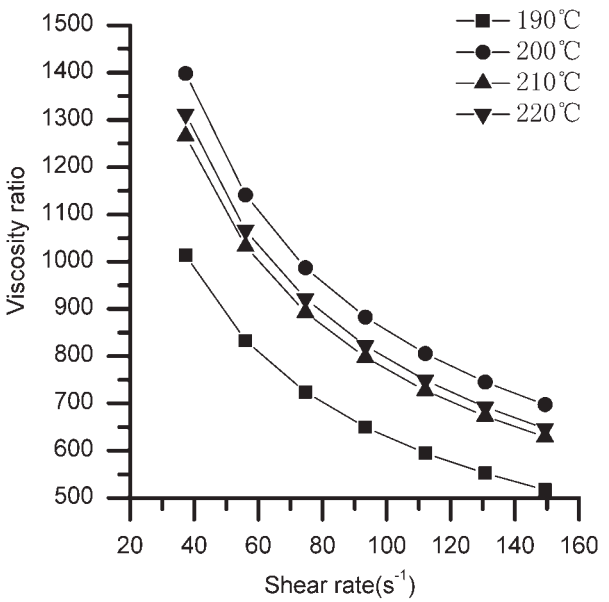

Figure 4 Viscosity ratio of Nylon 12 to PEG at different temperature and shear rate.

Figure 5 Process of morphology development in a binary immiscible polymer blends.

To lower the melting rate of the dispersed phase and make it possible to observe the morphological development, a low blending temperature of 190°C and low rotor speed of 50 rpm were selected. Figure 6 depicts the evolution of the phase size distribution as a function of the mixing time for the blend containing 25 wt % of Nylon 12. It shows that the nylon phase particles exhibited a triple-peak distribution. Even at the initial stage of mixing, about 3 min, in addition to particles of > 100 μm, a number of very small particles with a size of 0.1–10 μm were also produced in the system, as confirmed by the small droplets observed in Figure 7. Actually, according to the typical temperature curve with the time given in Figure 8, it took ~ 3 min to heat the sample to 180°C. Since the melting point of Nylon 12 is 178–180°C, at the end of 3 min Nylon 12 was just beginning to melt. From the sample obtained when the mixing time was only 3 min, we found, unexpectedly, that all the nylon had been dispersed in PEG and that that there was no nylon in the form of sheets or fibrils. Our result confirms the conclusion made by other investigators[3–5,16,25] that the most important deformation/disintegration processes took place within the first several minutes of mixing. Hence, even at an extremely high viscosity ratio of > 100, significant disruption of particles had occurred, unlike the Newtonian system in a shear flow field, which did not show breakup when the viscosity ratio was > 4.[16] This can be attributed to the fact that the elongation flow is much more effective in droplet breakup. Since the melting rate of nylon is very rapid, it remains difficult for us to trace the exact process by which the nylon pellets changed to small dispersed particles.

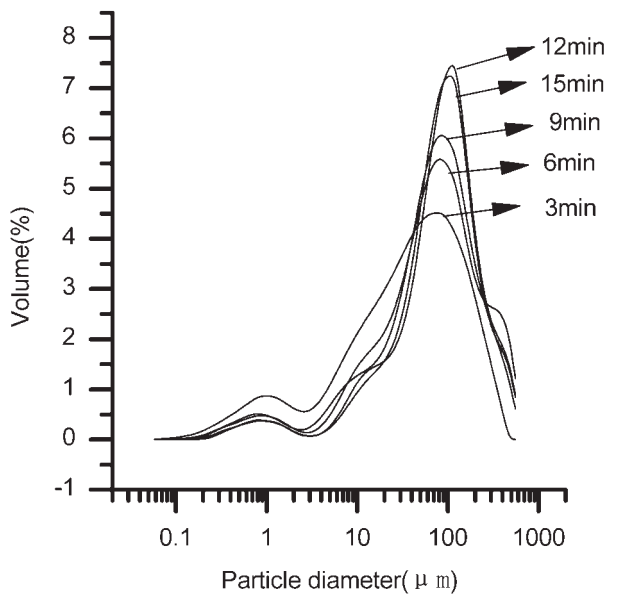

Figure 6 Size distribution of nylon phase at different blending time.

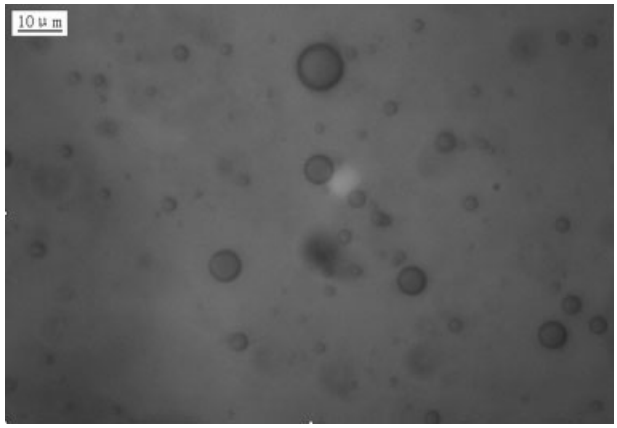

Figure 7 Optical micrograph of the nylon phase particles obtained after 3 min blending.

In addition, with increased mixing time, the number of very small particles (< 20 μm) decreased gradually, while the number of larger particles (> 20 μm) increased, and the peak on the right rose and became narrower; that is, as the mixing continued, the very small droplets would coalesce with each other and become larger ones, and the larger droplets produced in the early stage might also break up into smaller droplets. Through coalescence and the breakup process, the diameter difference between the particles in the system became smaller, and the distribution graph tended to be a single peak. Clearly there was an equilibrium size. Particles of that size would be stable in the system.

It should be mentioned that the peak of small particles with a diameter of 0.1–3 μm did not disappear even after 15 min. This might be attributable to the reduced efficiency of coalescence due to the greater hydrodynamic interaction of small particles.[18,29]

The reason for the triple peaks on the observed size distribution of the dispersed Nylon 12 particles remains unclear. It could have resulted from the effect of melting, breakup, and coalescence. It appears that the particles were formed according to more than one type of mechanism, which merits further investigation.

The decrease in uniformity with mixing time (Fig. 9) demonstrates that the size of the particles became more and more uniform. After 12-min processing, the value of uniformity remained nearly unchanged. From Figure 6 it can also be seen that the size distribution graphs at 12 min and at 15 min differ insignificantly from each other. Probably at this time the rates of

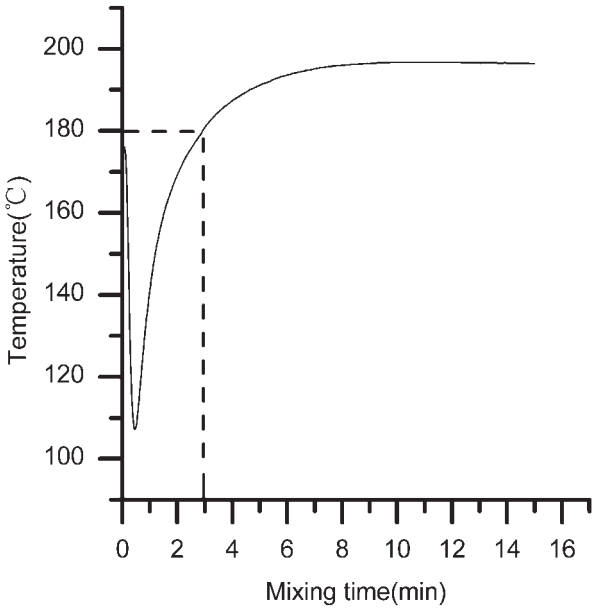

Figure 8 Typical temperature curve of the samples in the mixer.

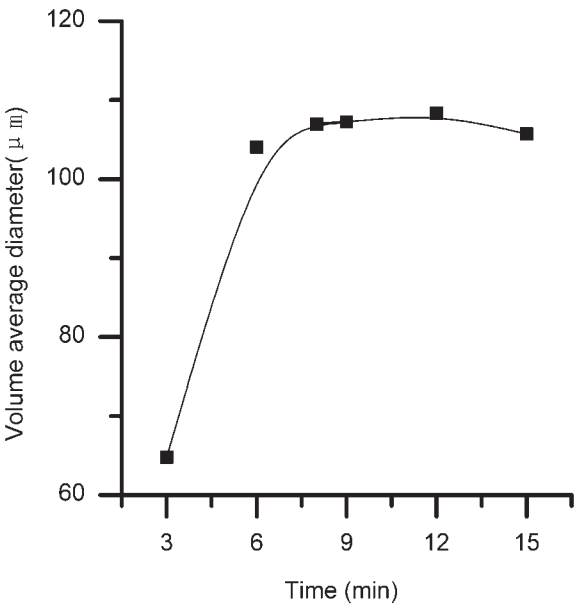

Figure 10 Volume-average diameter of the minor phase vs. mixing time at 190°C, 50 rpm and 25% weight fraction.

breakdown and coalescence of droplets were balanced and the equilibrium between breakup and coalescence was established.

Figure 10 shows that the volume average size of the particles first increased quickly with time, but then leveled off to a nearly constant value for the remainder of the mixing time. Apparently, this was because many small droplets that were produced during the early stage would coalesce with each other in the later period. This finding is contrary to the effect of mixing time on domain size reported in most studies,[27,30–32] in which the particle size either decreased gradually or remained practically unchanged with mixing time.

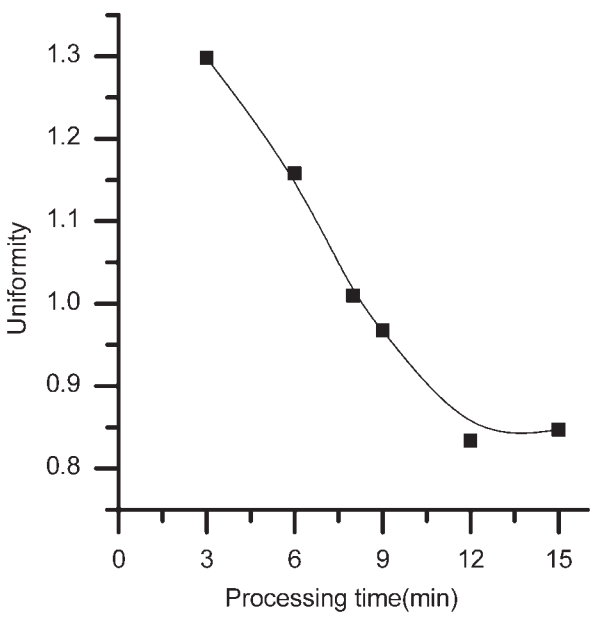

Figure 9 Size distribution of the minor phase at different mixing time at 190°C, 50 rpm and 25% weight fraction.

With respect to the dispersion process of the minor phase, some investigators considered the final morphology to be determined to a significant extent by the very early stage of mixing and observed that further mixing often had no or little impact on the morphology;[27] others reported that although significant changes in morphology occurred in the initial mixing stage, the final morphology of the minor phase depended mainly on the later mixing conditions after both components were molten.[28] Our results suggest that although increasing time had little effect on the average size of the minor phase after ~8 min, the size distribution still reduced and tended to be a single sharp peak over time. Evidently it takes more time to obtain a stable size distribution than to acquire a stable average size. Our experiments demonstrate that further mixing after the early stage also played an important role in the determination of final phase morphology, especially on the phase size distribution.

The main mechanism governing the morphology development is believed to be the dynamic equilibrium between the droplet breakup and coalescence; however, specific properties of these blends and processing conditions contribute to the difference in their morphological development. Li and Hu[23] studied the morphology development process of PP/PA6 blends and proposed that those different observation results in literatures were due to the different melting rate in those experiments. The higher melting rate caused by the more severe thermomechanical conditions employed

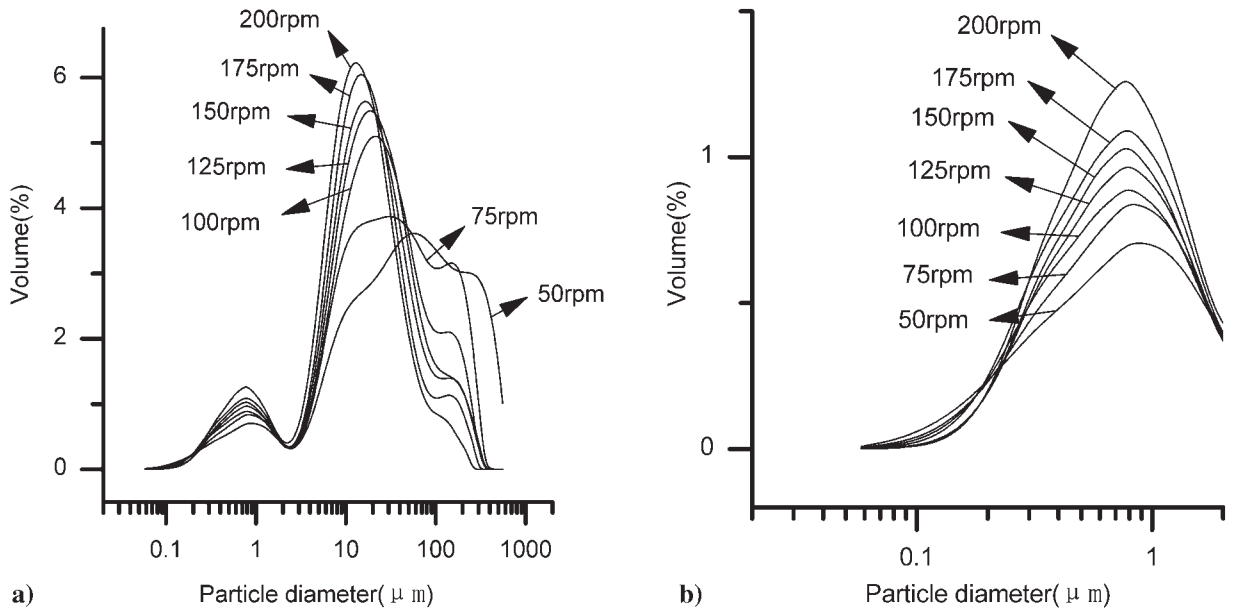

Figure 11 Effect of rotor speed on the size distribution of nylon phase in the blends containing 10 wt % nylon. (a) Change in size distribution; (b) magnified left small peak in the size distribution curve.

would make it more difficult to observe the coarsening process. In our results, it is of particular interest that the coarsening process was clearly observed even in the blend systems with the viscosity ratio of $\leq 10^2$–10^3, which could be attributed to the relatively low melting rate and the relatively low interfacial tension between the matrix and the dispersed phase. We calculate the surface free energy with the data reported in the literature. The surface free energy of polyethylene oxide (PEO) and PA 12 is 42.9 and 40.7 mN/m at 20°C,[33] respectively. The temperature coefficient of the surface free energy is −0.076 mN/(m K) for polyethylene oxide. We did not find the temperature coefficient of PA 12, so that of PA66, −0.065 mN/(m K) is chosen for our calculation. The calculated surface free energy of both PEO and PA 12 at 220°C is 27.7 mN/m. Since the two components exhibit equal surface free energy, it is reasonable to obtain a very low interfacial tension. This should aid the breakup process and help to observe the detailed morphology development of Nylon 12 in the

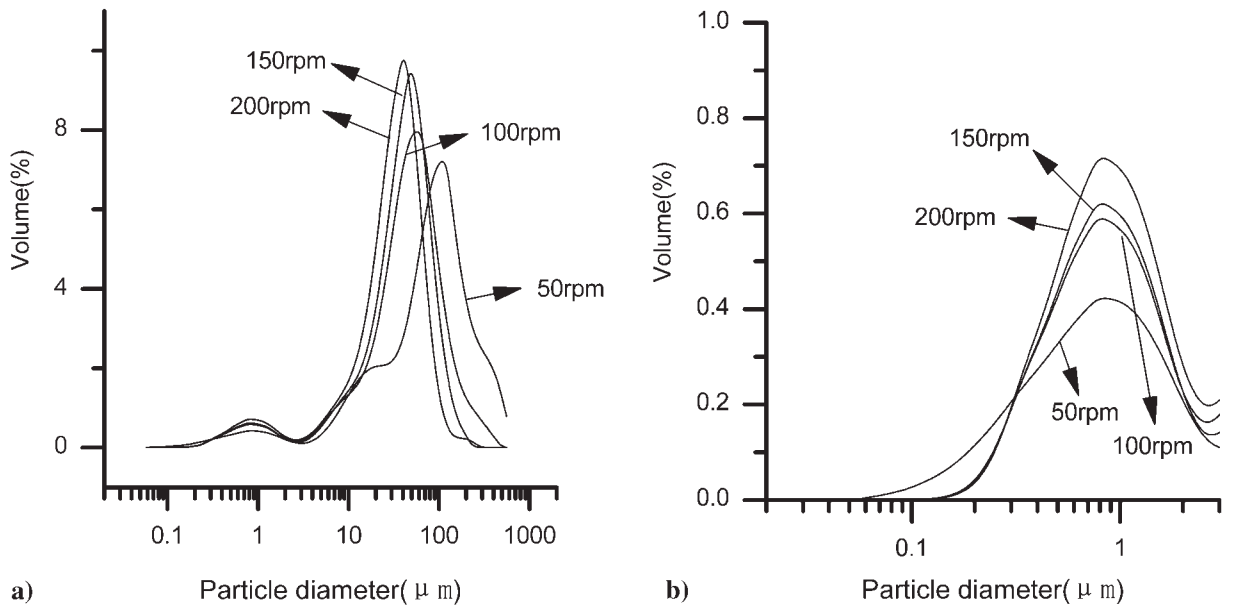

Figure 12 Effect of the rotor speed on the size distribution of nylon phase in the blends containing 25 wt % nylon. (a) Change in size distribution; (b) magnified left small peak in the size distribution curve.

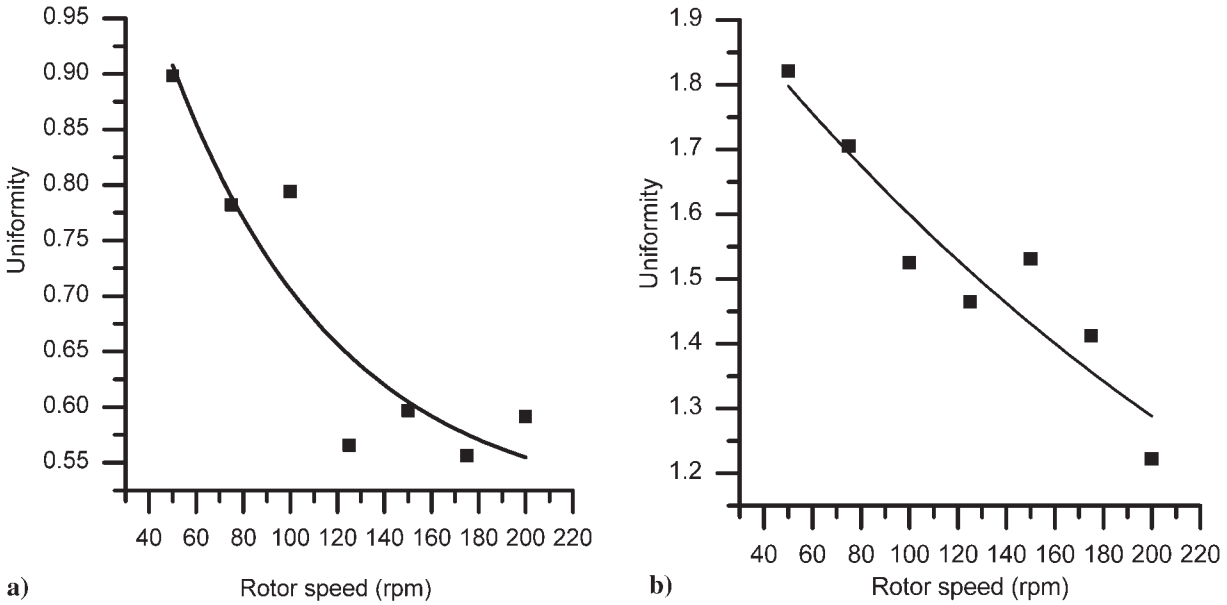

Figure 13 Effect of rotor speed on the uniformity of nylon particles. (a) Nylon 12, 25 wt %; (b) Nylon 12, 10 wt %.

matrix of PEG. In the early stage, under the complex shear field, the breakup of nylon pellets dominated the dispersion process. At this time many very small particles had been produced in the system, but the temporarily low coalescence rate made it possible to observe the particles of small size and the later coarsening process. As the number of small particles with a diameter less than equilibrium value increased, the rate of coalescence began to rise, and the process of coarsening replaced the breakup to be the dominant factor. Thereafter, the average size of droplets would increase gradually until a constant value was reached.

Everaert et al.[14] and Potschke et al.[24] concluded from their study that higher viscosity ratios hampered the droplet breakup process and that the flow field of the low viscous matrix was unable to transfer the applied shear stresses sufficiently to the highly viscous dispersed phase. In our experiments, although breakup could occur rapidly during the initial period, it was soon retarded and coalescence was facilitated as a consequence of the high mobility of dispersed domains in a low viscous matrix along with a higher coalescence probability. The equilibrium was set up rapidly due to the low viscosity of the matrix.

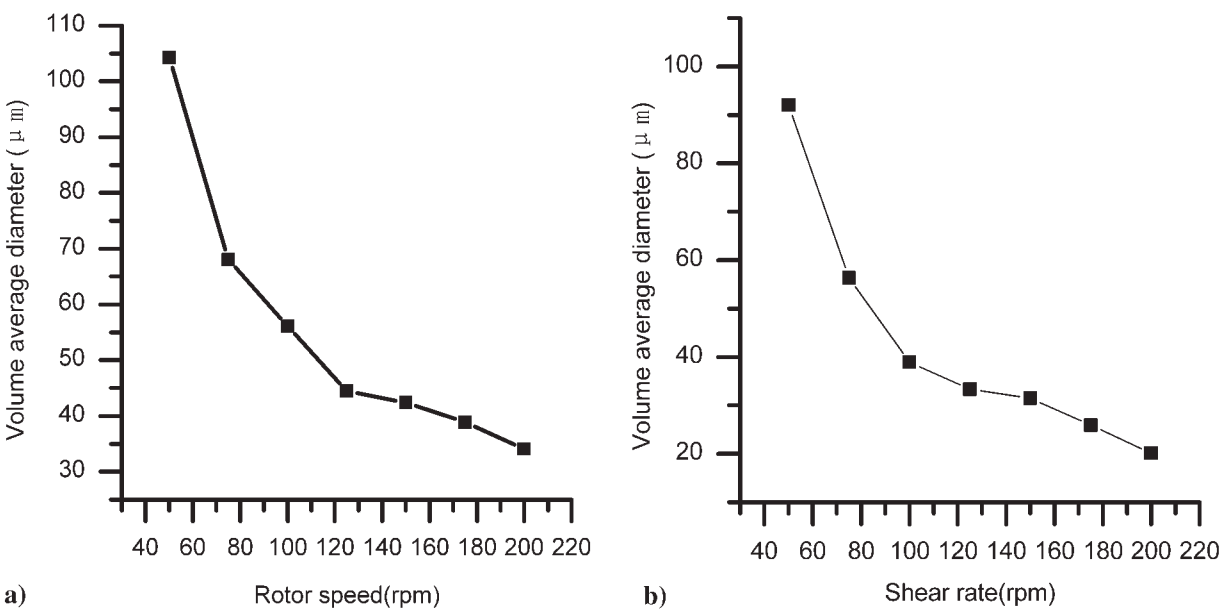

Figure 14 Effect of the rotor speed on the volume average size of nylon particles. (a) Nylon 12, 25 wt %; (b) Nylon 12, 10 wt %.

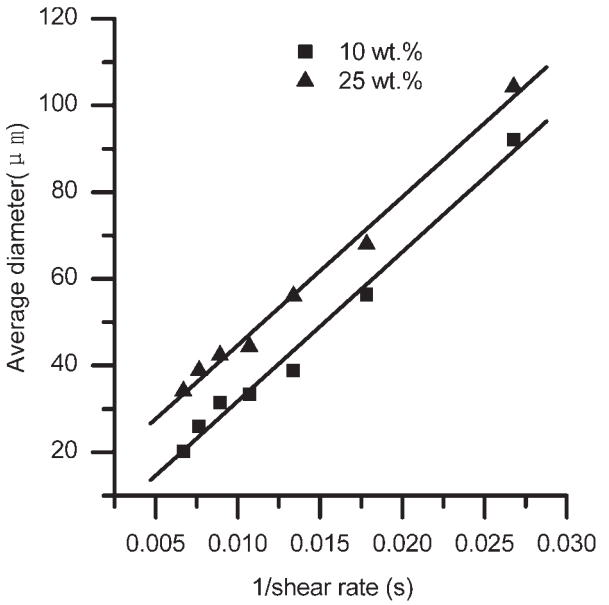

Figure 15 Particles average diameter versus reciprocal of shear rate at 10 wt % and 25 wt %.

Effect of rotor speed on particle size and size distribution

The influence of rotor speed on the size distribution of the two blends of 10% and 25% weight fraction is shown in Figures 11 and 12, respectively. The rotor speed was varied from 50 rpm to 200 rpm with an interval of 25 rpm. It is evident that in both systems the increasing rotor speed led to narrower size distribution. At the same time, the small peak on the left was found to be larger with the increased rotor speed. It can be understood that increased shear rate would result in both higher deforming forces and faster flow rate, thereby decreasing the collision time. Consequently, more and more small droplets were produced, while their coalescence probability was reduced. Figure 13 shows that the uniformity of the particle size was also reduced with the increasing rotor speed. This result might be due to the greater stress and increased energy input. When the rotor speed increases, the torque, which is considered to be proportional to the shear stress, increased as well. A blend subjected to a higher shear stress during the same period of mixing receives more energy input, so it is possible to reach the equilibrium between breakup and coalescence more rapidly and more closely, and for the particles obtained to be more uniform.

Influences of rotor speed on the particle size of two blends at 10% and 25% weight fraction were studied, and the results are shown in Figure 14(a,b), respectively. From both results, the average size of the particles decreased gradually with rotor speed. Also, the rate of size reduction slowed down as the rotor speed increased, especially when the rotor speed exceeded 100 rpm or so. These results are in agreement with Taylor's equation, which suggests a critical value of the Weber number below which no particle deformation takes place and, as a result, a critical particle size.

For most systems, droplet size was found to decrease with the increasing intensity of mixing,[11,22,34,35] while Favis[27] reported that the droplet size was independent of intensity of mixing. Fortelny et al.[12] observed that in the polyamide/[poly(phenylene oxide)+polystyrene] blend system the droplet size grew with the mixing rate at first and then began to decrease. These investigators attributed the different results to the dynamic equilibrium between breakup and coalescence of droplets; they concluded that the dependence of droplet size on rate of mixing was not necessarily a monotonic function for the blends with a high content of the dispersed phase. The relationship between shear rate and final droplet size has been theoretically proposed by Taylor, Wu, and Fortelny, who held that the size was inversely dependent on the shear rate. So we plot the phase size against the reciprocal of shear rate. The shear rate was estimated from the rotor speed. We find that both the results of 25% and 10% blends fit on linear curves very well, and the two lines paralleled with each other (Fig. 15). The difference in the weight fraction of nylon phase does not alter the slope of the fitted line, but only affects the value of the intercept of the line. This result demonstrates that Fortelny's equation [eq. (3)] is a good predictor of the relationship between the dispersed phase size and shear rate for our system. In his equation, when the temperature and the components of the system are fixed, the coefficients in the first

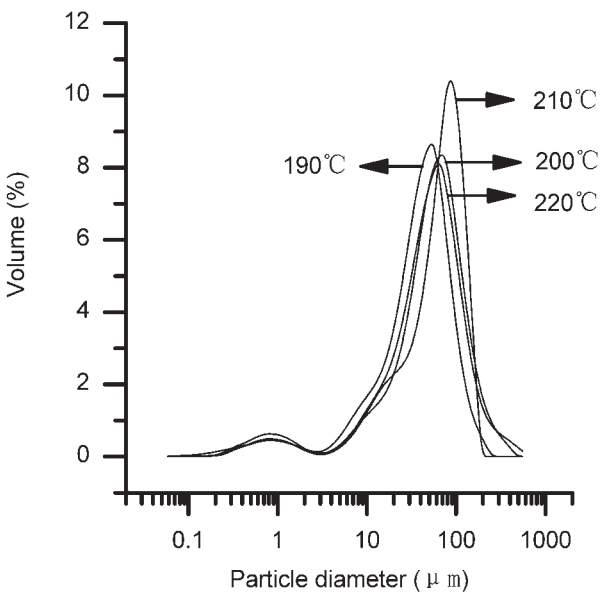

Figure 16 Size distribution of nylon phase in the blends containing 25 wt % nylon at different temperature with rotor speed at 100 rpm.

item on the right will remain constant, so the particle diameter will be inversely proportional to the shear rate. The concentration of the minor phase influences only the second item on the right.

Effect of temperature on particle size

Blending experiments were conducted at four temperatures; the dependence of the dispersed phase size on temperature is shown in Figures 16 and 17, respectively. It can be seen in Figure 17 that the size at 190°C is smaller than the value at the other three temperatures, and when the temperature is 200–220°C, the values of particle size are nearly constant. The distribution curve in Figure 16 shows that differences exist in the size distribution at selected four temperatures and the size distribution at 210°C is more uniform, as reflected in the values of the uniformity of the size distribution at the four temperatures in Figure 18. The experiments were repeated, and the same results were obtained.

Since the temperature coefficient of surface tension is very low at tested temperatures for Nylon 12 and PEG, the surface tension of the two components changes very little at these temperatures, and their interfacial tension, determined by their surface tension and polarity, will also remain nearly unchanged. Thus, temperature will only influence the viscosity of the two components and their viscosity ratio. The change of viscosity will be responsible for all the difference in size and size distribution. The variation in the viscosity ratio of Nylon 12/PEG with the temperature is shown in Figure 4. At 190°C, the viscosity ratio is relatively low, and the viscosity ratio at 200°C is slightly higher than that at other temperatures. We can observe in Figure 15 that the average size is low at 190°C, reaches the highest value at 200°C, and remains almost the same at 210°C and 220°C. The variation in the average size corresponds exactly to the change in the viscosity ratio. A lower viscosity ratio will lead to smaller particle size, which is in good agreement with the theory of Wu[11] and Everaert et al.,[14] who indicated in their theoretical equations that the viscosity ratio will significantly affect the average size of the minor phase and that the closer viscosity of the components will lead to a smaller minor phase size.

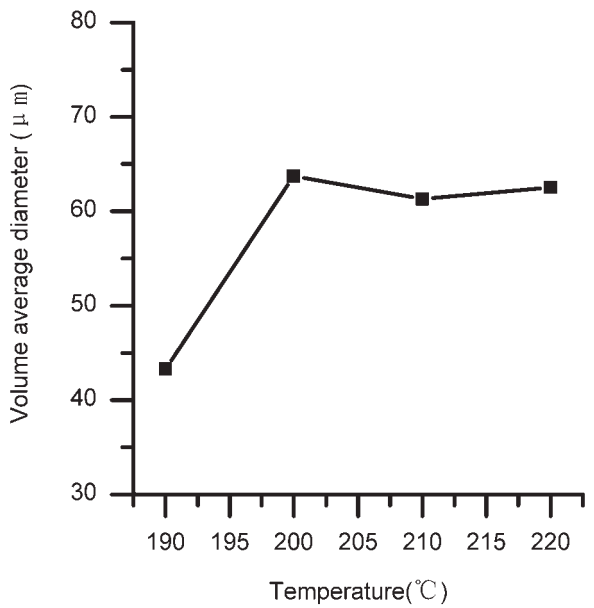

Figure 17 Volume-average size of nylon particles vs. temperature at 100 rpm and a mixing time of 8 min.

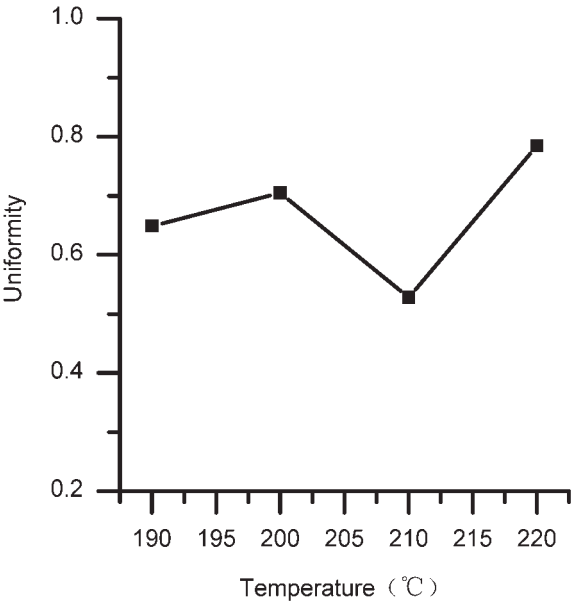

Figure 18 Size distribution at different temperature at 100 rpm and a mixing time of 8 min.

CONCLUSION

The phase morphology development in the Nylon 12/PEG blend with an extremely high viscosity ratio was investigated. Laser scattering was applied to measure the size and size distribution of the minor phase as functions of mixing time, rotor speed, and mixing temperature. Nylon 12, as the minor phase, was found to form spherical particles in the PEG matrix. Many small particles of 0.1–10 μm were observed in the initial stage of processing, which demonstrated that the major breakdown of pellets occurred at the very beginning. The volume average size increased with the time in the initial period and then leveled off. The size distribution of the dispersed phase narrowed with prolongation of the mixing time and tended to be a single narrow peak.

The dispersed phase size was significantly affected by the rotor speed within the range of 50–200 rpm. The fitting results showed that the diameter of the dispersed particles was inversely proportional to the

shear rate, with the slope of the fitted line independent of the volume ratio of the dispersed phase. The phenomenon is in good agreement with the equations proposed by Taylor, Wu, and Fortelny, and others. By affecting the viscosity ratio, the temperature also had a considerable effect on the size and size distribution of the dispersed phase. Lower viscosity ratio led to smaller particle size.

APPENDIX: ESTIMATION OF SHEAR RATE IN HAAKE RHEOMIX 600p MIXER

Mixer chamber radius	$R_a = D_a/2 = 19.65$ mm
Maximal radius of rotors	$r_1 = 18.2$ mm
Minimal radius of rotors	$r_2 = 11.0$ mm
Maximal slot	$y_1 = 8.6$ mm
Minimal slot	$y_2 = 1.4$ mm
v_1	Tangential velocity at the radius of r_1
v_2	Tangential velocity at the radius of r_2
Maximal shear rate	$\dot{\gamma}_1 = v_1/y_1 = 2r_1\pi n/y_1$
Minimal shear rate	$\dot{\gamma}_2 = v_2/y_2 = 2r_2\pi n/y_2$
Average shear rate	$\dot{\gamma} = (\dot{\gamma}_1 + \dot{\gamma}_2)/2$

References

1. Paul, D. R.; Newman, S. Polymer Blends; Academic Press: New York, 1978; Vol. 1, Chapter 1, p 11.
2. Folkes, M. J.; Hope, D. S. Polymer Blends and Alloys; Blackie: London, 1993.
3. Sundararaj, U.; Macosko, C. W. Macromolecules 1995, 28, 2647.
4. Elmendorp, J. J.; van der Vegt, A. K. Polym Eng Sci 1986, 26, 1332.
5. Scott, C. E.; Macosko, C. W. Polym Bull 1991, 26, 341.
6. Sundararaj, U.; Macosko, C. W.; Rolando, R. J.; Chan, H. T. Polym Eng Sci 1992, 32, 1814.
7. Ghodgaonkar, P. G.; Sundararaj, U. Polym Eng Sci 1996, 36, 1656.
8. Utracki, L. A.; Shi, Z. H. Polym Eng Sci 1992, 32, 1824.
9. Huneault, M. A.; Shi, Z. H.; Utracki, L. A. Polym Eng Sci 1995, 35, 115.
10. Zhang, Z. Y.; Qiao, J. L. Polym Eng Sci 1991, 31, 1553.
11. Wu, S. Polym Eng Sci 1987, 27, 335.
12. Fortelny, I.; Cerna, Z.; Binko, J.; Kovar, J. J Appl Polym Sci 1993, 48, 1731.
13. Willemse, R. C.; Ramaker, E. J. J.; van Dam, J.; de Boer, A. P. Polymer 1999, 40, 6651.
14. Everaert, V.; Aerts, L.; Groeninckx, G. Polymer 1999, 40, 6627.
15. Chung, O.; Coran, A. Y. Rubber Chem Technol 1997, 70, 781.
16. Taylor, G. I. Proc R Soc London, Ser A 1934, 146, 501.
17. Taylor, G. I. Proc R Soc London, Ser A 1932, 138, 41.
18. Zeichner, G. R.; Schowalter, W. R. AIChE J 1977, 23, 243.
19. Jana, S. C.; Sau, M. Polymer 2004, 45, 1665.
20. Bu, W. S.; He, J. S. J Appl Polym Sci 1996, 62, 1445.
21. Schreiber, H. P.; Olguin, A. Polym Eng Sci 1983, 23, 129.
22. Nair, S. V.; Oommen, Z.; Thomas, S. J Appl Polym Sci 2002, 86, 3537.
23. Li, H. X.; Hu, G. H. J Polym Sci Part B: Polym Phys 2001, 39, 601.
24. Potschke, P.; Wallheinke, K.; Fritsche, H.; Stutz, H. J Appl Polym Sci 1997, 64, 749.
25. Thomas, S.; Groeninckx, G. J Appl Polym Sci 1999, 71, 1405.
26. Grace, H. P. Chem Eng Commun 1982, 14, 225.
27. Favis, B. D. J Appl Polym Sci 1990, 39, 285.
28. Bourry, D.; Favis, B. D. Polymer 1998, 39, 1851.
29. Wang, H.; Zinchenko, A. Z.; Davis, R. H. J Fluid Mech 1994, 265, 161.
30. Hu, G. H.; Kadri, I. J Polym Sci Part B: Polym Phys 1998, 36, 2153.
31. Karger-Kocsis, J.; Kallo, A.; Kuleznev, V. N. Polymer 1984, 25, 279.
32. Scott, C. E.; Macosko, C. W. Polymer 1994, 35, 5422.
33. http://www.surface-tension.de/solid-surface-energy.htm.
34. Grizzuti, N.; Bifulco, O. Rheol Acta 1997, 36, 406.
35. Takahashi, Y.; Imura, N.; Miyanishi, K.; Kitade, S.; Noda, I. Mater Sci Res Int 2003, 9, 278.